Local B_1 Shimming for Imaging the Prostate at 7 Tesla

G. J. Metzger[1], P-F. Van de Moortele[1], C. J. Snyder[1], J. T. Vaughan[1], and K. Ugurbil[1,2]

[1]Center for Magnetic Resonance Research, University of Minnesota, Minneapolis, MN, United States, [2]Hochfeld-Magnetresonanz-Zentrum, Max Plank Institut für Biologische Kybernetic, Tübingen, Germany

INTRODUCTION: The ability to image the body at ultra high field (UHF) is made difficult by the presence of destructive interferences which result in an inhomogeneous transmit B_1 (B_1^+) (1,2). These destructive interferences play an increasing role as the radiofrequency (RF) wavelength, which is proportional to the static magnetic field, becomes smaller than the object of interest. At 7 Tesla, the wavelength of RF in human tissues is approximately 12 cm which results in the creation of complex B_1^+ fields. In this work, we demonstrate the application of local B_1 shimming to minimize these destructive interferences in a region around the prostate. This application uses subject specific measurements to map the relative transmit phases of each channel of an eight element stripline transverse electromagnetic (TEM) transceive coil in order to minimize destructive interferences in a focal region (3). The methods proposed make more efficient use of available B_1^+ thus minimizing the deposition of RF energy which is also an issue of major concern with increasing field strength. While the use of B_1 shimming in general is necessary for developing UHF imaging applications, the local B_1 shimming employed here is particularly advantageous for imaging a focal region of interest without the need for complicated calibration measurements or hardware.

METHODS: The MRI systems used for this study included a Magnex 7T, 90cm bore magnet with Siemens console and whole body gradients. For transmit, a custom 8 kW amplifier was passed into the standard Siemens control software to provide power monitoring. All acquisitions complied with FDA guidelines for specific absorption rates (SAR) and gradient duty cycle. The single RF transmit channel was passed through an 8 way splitter (Werlatone Inc., Brewster, NY, USA) where each channel was subsequently connected to a phase shifter (ATM Microwave, Patchogue, NY). The transceiver coil used was a flexible 8 channel stripline TEM design with 4 elements mounted on both anterior and posterior flexible PTFE plates.

Imaging studies consisted of anatomic T1W gradient echo (GRE) and respiratory triggered T2W turbo spin echo (TSE) images along with B_1^+ mapping and B_1 shimming acquisitions. All sequences were acquired both before and after calculation and implementation of the subject dependent phase corrections determined by the local B_1 shimming procedure. The T1W GE anatomic images were acquired with the following parameters: matrix = 320x320, field of view (FOV) =34 cm, flip angle = 10º, slice thickness = 5 mm, TR=40 ms and TE= 3.68 ms. The respiratory triggered TSE images were acquired with the following parameters: refocusing pulse = 120 degrees, echo train length = 13, matrix = 256x256, FOV = 220 mm, slice thickness = 5 mm and TE = 102 ms . Mapping of the transmit B_1 was accomplished with a two flip angle approach; FOV = 300 mm, TR = 6 s, TE = 4.1 ms, matrix = 128x128, 5 mm slice thickness and flip angles of 30 and 60 degrees.

Subject dependent B_1 shimming was implemented by first acquiring a series of low resolution T1-weighted gradient echo images covering the anatomy of interest with a common phase across all channels: FOV = 300 mm, flip angle = 10º, TR = 100 ms, TE = 4.1 ms, matrix = 128x128, slice thickness = 5 mm. This sequence was used to obtain 8 complex images ($\mathbf{C}_j$) where each image was acquired by transmitting through a single transmit channel while averaging over all eight channels on receive. The common phase terms of $\mathbf{C}_j$ were removed by dividing by the complex data of the first transmit channel resulting in normalized complex images ($\mathbf{Cn}_j$) , $\mathbf{Cn}_j = \mathbf{C}_j / \mathbf{C}_1$. Local B_1 shimming was performed by averaging the phase of each channel over a common region of interest (ROI) and then subtracting the normalized phase from the respective channel to minimize the destructive phase cancellation and maximize the available B_1^+. The ROI around the prostate used for shimming is shown by the black curve **(Fig. 1a)**.

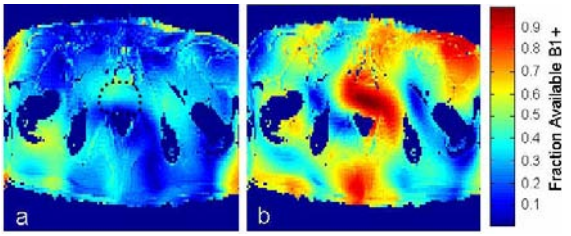

Fig. 1: Maps of the fractional available B_1^+ before (a) and after (b) local B_1 shimming. Increased B_1^+ efficiency is predicted in (b) after adjusting the phases of the eight transmit channels.

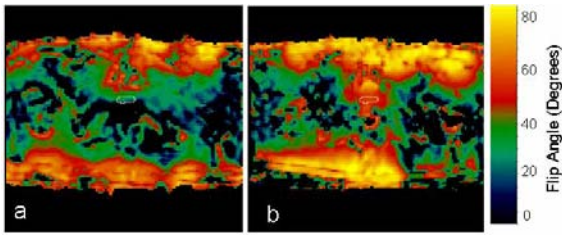

Fig.2: B_1 maps before (a) and after (b) local B_1 shimming. Increased transmit efficiency and homogeneity are demonstrated in the regions of the prostate.

RESULTS AND DISCUSSION: The most efficient theoretically possible combination of the transmit B_1 phases from multiple elements is given by the sum of the magnitude (SOM) of $\mathbf{Cn}_j$. However, in practice, the best possible outcome with a transmit array coil involves the simultaneous use of all coil elements which is represented by the complex superposition of the $\mathbf{Cn}_j$ given as the magnitude of the sum (MOS). The ratio of MOS to SOM yields the fraction of available B_1^+ and provides an intuitive index for visualizing the effectiveness of B_1 shimming **(Fig. 1)**. In this example the available B_1 in the prostate is predicted to increase from 33% to 96% within the prostate after applying transmit channel phase corrections of 145, 269, 323, 204, 0, 32, 201, and 42 degrees for channels 1 through 8 respectively. The measured B_1^+ maps confirm the increased efficiency in delivered B_1^+ along with improved B_1^+ homogeneity over the prostate **(Fig. 2)**. For a given applied transmit power the flip angle mean and standard deviation over the prostate before and after B_1 shimming were 23.8 ± 8.0 and 53.3 ± 1.9 degrees, respectively. With improved efficiency and homogeneity over the prostate high quality images of the prostate can be obtained (**Fig. 3**). Both the GRE and TSE images show homogeneity in signal intensity across the anatomy of interest while the T2W TSE image shows the expected contrast allowing easy identification of prostate morphology: urethra (Ur), transition zone (Tz), peripheral zone (Pz), neurovascular bundle (Nv) and rectum (R).

While tremendous B_1^+ inhomogeneities exist in body imaging at UHF, the respectively small volume of the prostate enables a simple phase based optimization to achieve excellent results without the need for more complicated calibration measurements or hardware. The minimization of destructive interferences through local phase based B_1 shimming resulted in the acquisition of high quality GRE and TSE prostate images at 7 Tesla. In general, these results demonstrate the utility of local B1 shimming to improve focal UHF applications.

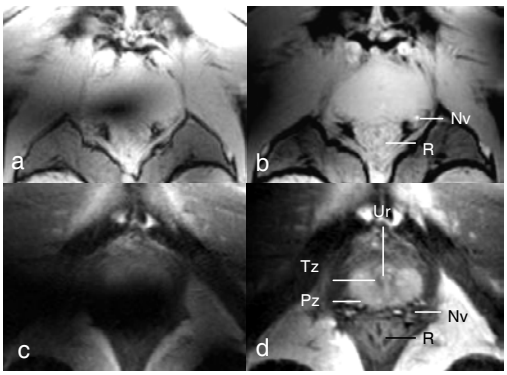

Fig. 3: Anatomic images zoomed in on the prostate. T1W GRE images before (a) and after (b) B_1 shimming. T2W TSE images before (c) and after (d) B_1 shimming.

REFERENCES: [1] Van de Moortele et al. MRM 2005; 54(6):1503-1518 [2] Vaughan JT et al. Proc. of the 14th meeting of the ISMRM 2006; 213 [3] Van de Moortele et al. International Symposium on Biomedical MRI and Spectroscopy at Very High Field 2006

ACKNOWLEDGEMENTS: Supported by NIH Grants P41 RR08079; The 7 Tesla system acquisition was funded by the Keck Foundation, NSF grant 9907842, NIH grant R01 EB000895-04, and NIH grant S10 RR1395